BULLETIN OF THE POLISH ACADEMY OF SCIENCES
TECHNICAL SCIENCES, Vol. 63, No. 4, 2015
DOI: 10.1515/bpasts-2015-0110

Miniature size multiband planar patch antenna fabricated on a bioplastic substrate

M.R. AHSAN[1]*, M.T. ISLAM[1], M. HABIB ULLAH[2], H. ARSHAD[3], and M.T. ALI[4]

[1] Department of Electrical, Electronic and Systems Engineering, Faculty of Engineering and Built Environment, Universiti Kebangsaan Malaysia (UKM), Bangi, Selangor, Malaysia
[2] Department of Electrical Engineering, Faculty of Engineering, University of Malaya (UM), Kuala Lumpur, Malaysia
[3] School of Information Technology, Faculty of Information Science and Technology, Universiti Kebangsaan Malaysia (UKM), Bangi, Selangor, Malaysia
[4] Antenna Research Group, Microwave Technology Centre, Faculty of Electrical Engineering, Universiti Teknologi Mara (UiTM), Shah Alam, Selangor, Malaysia

Abstract. In this article, a simple design of rectangular microstrip feed planar antenna with wide arcs and square shape slot is proposed for Radio Frequency Identification (RFID), Worldwide Interoperability for Microwave Access (WiMAX) and C/X-band wireless communications. The prototype of the antenna has been fabricated 1.0 mm thick ceramic filled bioplastic substrate by using optimal dimension obtained from design/simulations and antenna performances are experimentally tested. The experimental results confirm the impedance bandwidths for S11≤ -10 dB are of 712 MHz (0.355–1.067 GHz), 1.38 GHz (2.92–4.3 GHz) and 2.46 GHz (6.55–9.01 GHz) for 0.788, 3.34 and 8.01 GHz band respectively. The proposed antenna shows almost steady and symmetrical radiation patterns for all three bands with the maximum gains of 1.37, 2.8 and 3.56 dBi respectively. Based on the antenna performances, it can successfully cover the frequency band requirement for RFID, WiMAX and C/X-band applications.

Key words: bioplastic substrate material, multiband antenna, planar patch antenna, RFID, C/X band, WiMAX application.

1. Introduction

During the past couple of years, the researchers have paid their best efforts in designing antennas of wideband, working at multiple frequencies while maintaining the compactness of the module. The microstrip antennas are vastly used for their compact size, less complex structure, simple manufacturing process, easy integration ability with other devices and components. However, they also suffer from unexpected feed radiation, narrow impedance bandwidth, higher cross polarization which needs to improve by using efficient designing techniques of the antennas [1, 2]. The recent literatures suggest adding extra resonators [3], using meandered strips [4], applying aperture coupled feed [5], employing thick dielectric substrate [6], modifying the ground plane [7] and so forth.

Multiple frequency bands from the single antenna module have attracted many researchers due to their substantial applications in wireless communications, mobile/cellular network, WiMAX, satellite communications, synthetic aperture radar, etc. Reviewing recently published literatures have suggested numerous approaches to realize more than one frequency band out of a single antenna module. As, for example, introducing artificial magnetic conductor [8], implementing fractal structures [9], cutting slots of different shapes and sizes on the radiating patch [10, 11], constructing electromagnetic bandgap (EBG) structure [12], adding stubs or parasitic elements [13], feeding through coplanar waveguide [14], using defected/reformed ground plane [15] and so on. The air exposure of the substrate by etching out the part of copper layer is an efficient and easy to apply technique in the design and fabrication process. In order to overcome the limitations and meet the growing demands of multi-band functionality, a suitable microstrip patch antenna of simple geometrical structure with reduced dimension and light weight has to be designed by exploiting the potentialities of latest technology.

This paper offers designing and realization of compact multi-band microstrip planar antenna on custom-made bioplastic dielectric substrate for serving the ubiquitous wireless communications in the RFID, 3.5 GHz WiMAX and C/X-band frequencies. The performances of antenna have been explored in terms of reflection coefficient, gain and radiation patterns and measured in a standard anechoic chamber. A physical module of the proposed antenna has been developed by using the optimized parameters obtained from successful numerical simulations. It has been found that the fabricated antenna maintains appreciable electrical properties like wide band, almost symmetric and steady radiations, low cross-polarizations and adequate gain.

2. Geometry and design of proposed antenna

The detail geometrical configuration of the proposed multiband planar microstrip antenna is presented in Fig. 1. The proposed antenna is printed on custom-made ceramic filled

*e-mail: rezwanul.ahsan@yahoo.com

composite bioplastic substrate material with dielectric constant $\varepsilon_r = 10.0$, $\tan(\delta) = 0.002$ and overall dimension is $24 \times 17 \times 1$ mm^3. The substrate material has been constructed by arranging layers of bioplastic substances and ceramic power according to the desired material property. Three different types of ceramic filled bioplastic substrate materials are formed by applying different compositions; namely bio-10 ($\varepsilon_r = 10.0$), bio-12 ($\varepsilon_r = 12.0$) and bio-15 ($\varepsilon_r = 15.0$). The assorted ceramic powder with polymeric binder has sintered using polymeric sponge method. In between the 0.25 mm thick bioplastic sheet created from organic biomass sources, required amount of ceramic power layer has been introduced with a binder to form bioplastic-ceramic-bioplastic sandwich structure. After using the multi-press machine, the final bioplastic composite material substrate is prepared with standard 35.0 μm thick copper lamination on both sides.

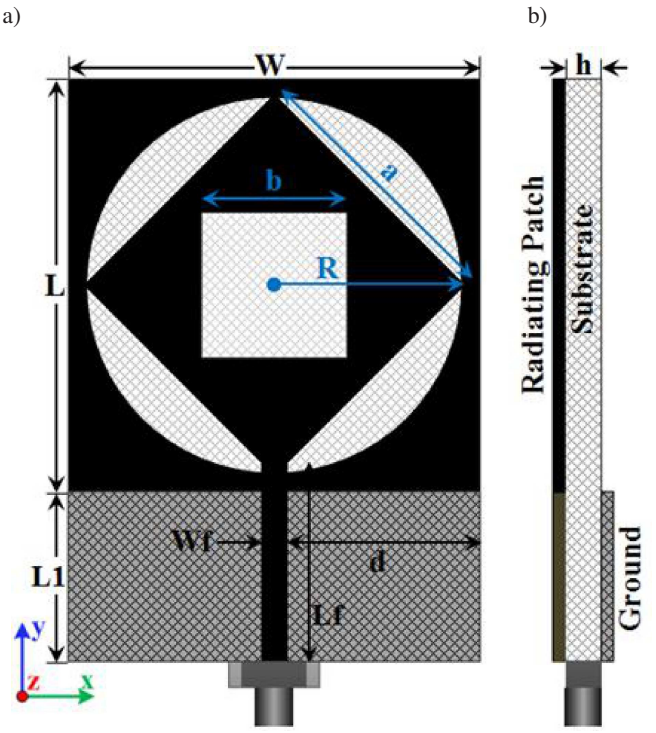

Fig. 1. Geometrical structure of the proposed antenna (a) top view and (b) side view

The commercially available full-wave electromagnetic (EM) field solver namely high frequency structural simulator (HFSS) is used for working with design and optimization processes [16]. Initially the dimension of the antenna and patch are estimated by using the standard formulation available in literatures [1]. The mathematical formulation defines that, the patch of L long (along the plane of feed line) can be estimated as:

$$L \approx 0.49\lambda_d = 0.49\frac{\lambda}{\sqrt{\varepsilon_r}}, \tag{1}$$

where λ_d is the wavelength of a wave in a large block dielectric with ε_r and λ is the free-space wavelength at resonance.

The width of the patch, W is responsible for providing the adjustment of input resistance, can be calculated for the experimental hardware model as:

$$W = \frac{\lambda}{2}\sqrt{\frac{\varepsilon_r + 1}{2}}. \tag{2}$$

Due to the fringing effect, the resonant length of the patch is reduced and more accurately can be expressed as:

$$L = 0.5\frac{\lambda}{\sqrt{\varepsilon_r}} - 2\Delta L, \tag{3}$$

where ΔL is the fringing length, given by:

$$\Delta L = 0.412\frac{(\varepsilon_{re} + 0.3)\left[\frac{W}{t} + 0.264\right]}{(\varepsilon_{re} - 0.258)\left[\frac{W}{t} + 0.8\right]}t, \tag{4}$$

where ε_{re} is the effective dielectric constant, can be written as:

$$\varepsilon_{re} = \frac{\varepsilon_r + 1}{2} + \frac{\varepsilon_r - 1}{2}\left(1 + \frac{10t}{W}\right)^{-0.5}. \tag{5}$$

The total fringing length, $2\Delta L$ is accounted for both edge of the patch and patch length should be reduced below half wavelength to attain desired resonance. Furthermore, the stated Eqs. (1)–(5) are suitably applied for rectangular patch only and the geometric structure/dimension of the proposed antenna has achieved through various numerical simulations, on test/modify/run basis.

The simple geometrical structure of the patch has been formed by using the combination of circle, rhombus and square geometry. The radiating element of the patch antenna is fed by a 1.2 mm wide and 8 mm long microstrip line that efficiently comply with the 50 Ohm input impedance. A numbers of numerical simulations have been performed to determine the optimized parameters for the antenna with HFSS. The optimized parameters for the proposed antenna are listed in Table 1.

Table 1
Optimized parameters of the proposed multiband antenna

Param.	Value (mm)	Param.	Value (mm)
W	17	L	17
Wf	1.2	$L1$	7
d	7.9	Lf	8
R	8	h	1
a	11.3	b	6

3. Parametric investigations

By cutting slots of various geometrical shapes at radiating element assist in lowering down the resonant frequency and help to substantially reduce the overall dimension of the antenna. Some of the parametric studies are performed on the geometrical design of proposed antenna to obtain the optimal dimensions where the best impedance matching is occurred. Since the complete size of the antenna and feed location has considerable effect on the antenna performances, they are not

included in the parametric investigation. To understand the effect of different parameters on the antenna performances (in terms of S11), only one item has been chosen for the study while the remaining items left constant.

The design of the proposed multi-band antenna has started by choosing the estimated dimension of the rectangular shaped radiating element by following the analytical studies through EM simulation software. Figure 2 shows the gradual steps involve in obtaining the final geometrical structure of the proposed antenna and their corresponding frequency responses are illustrated in Fig. 3. For the Ant.1, the resonant frequency is seen to cross over -10 dB value at around 2.01 GHz and 8.12 GHz. Inserting the wide circular slot at the center of the square shape radiator (Ant.2) changes the current direction and density, which may assist in achieving less than -10 dB frequency resolution clearly visible at two points centered at near 1.0 GHz and 7.8 GHz. Whereas, the S11 curve is seen to just cross at around 4.62 GHz with the value of -11.18 dB.

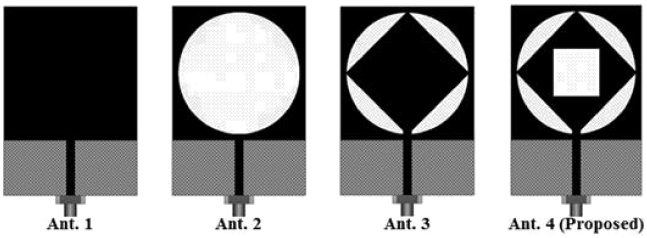

Fig. 2. Steps involved in designing the proposed antenna

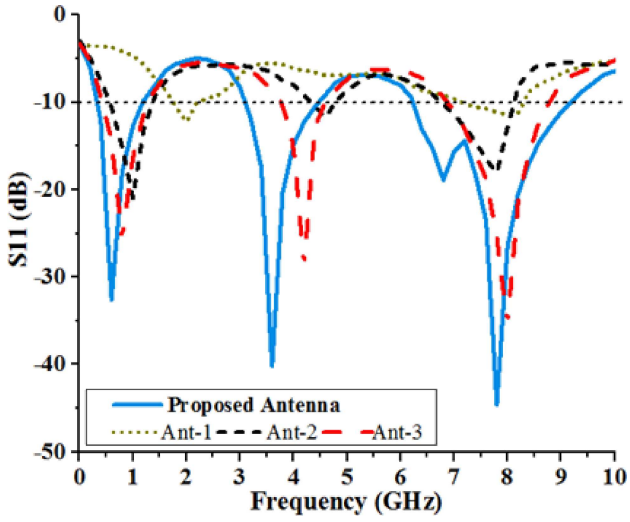

Fig. 3. Frequency response of different geometrical structure of the proposed antenna

Through inductive loading by adding rhombus shape at the center of the circle has increased the overall radiating areas as well as four capacitive effect due to the arc shape slots are introduced. Due to the inductive and capacitive loading on the effective radiating dimension, the perturbed surface current direction and intensity may help to produce the resonant frequency at 0.77, 4.22 and 8.02 GHz with reflection coefficient (S11) of -25.1, -28.22 and -34.56 dB for lower, middle and upper working band respectively. By cutting relatively wide square slot at the center of the rhombus has made the operating frequency band to shift toward the lower frequency as expected. By wisely setting the optimized dimension of the square shape slot, the desire resonant frequencies with improved -10 dB impedance bandwidths and less reflection coefficients have achieved. The simulation results for the proposed antenna for different geometrical configurations are presented in Fig. 3, where the achieved impedance bandwidths are of 0.335 to 1.086 GHz, 3.1 to 4.46 GHz and 6.27 to 9.2 GHz with reflection coefficient -32.57 dB, -40.22 dB and -44.7 dB for resonant frequency centered at 0.651, 3.51 and 7.83 GHz respectively.

The simulation software is used to study the effect of varying the radius of circular slot and length of its associated rhombus element and their combined effect is shown in Fig. 4. The successive reduction of radius and length of rhombus increases the area of radiating element and leads to shifting the resonant modes towards the higher frequency and vice versa. The numerical analysis found that the circle radius of $R = 8.0$ mm and side length of rhombus $a = 11.31$ mm would yield best impedance matching and help to achieve desired resonant frequency and bandwidth.

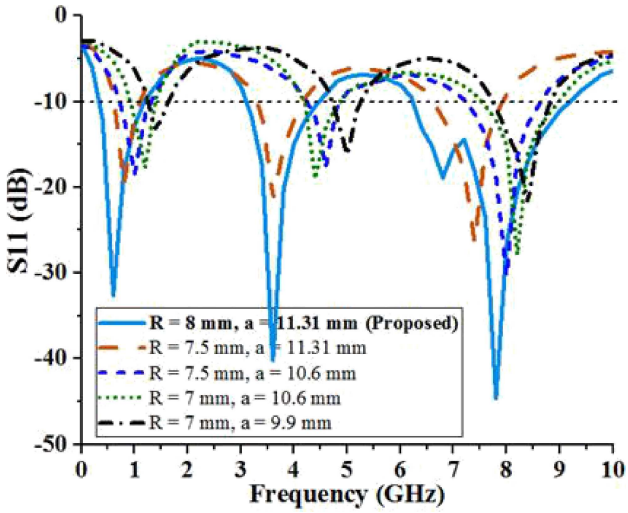

Fig. 4. Effect of varying radius of circle and side length of rhombus on the bandwidth and reflection coefficient (S11)

Further study is proceed with optimizing the dimension of central square slot and the variation of reflection coefficients are shown in Fig. 5. The figure demonstrates that the lower and middle frequencies are least affected due to the change of side length of central square, and the higher frequency band is mostly affected. Inclusion of wide square slot inside the rhombus radiating element would create a capacitive effect and certainly perturbed the intensity and the effective length of current paths. Due to the fairest impedance matching at $b = 6.0$ mm, wide bandwidth is achieved at the upper frequency band through merging of two frequency bands with a slight shift towards lower frequency.

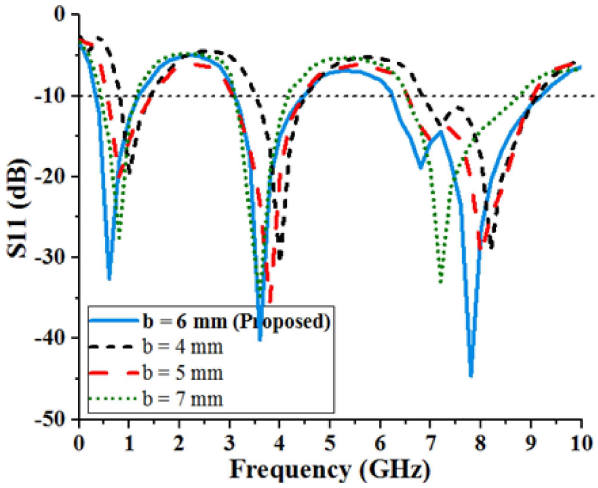

Fig. 5. Effect of length of central square slot on the bandwidth and reflection coefficient (S11)

The parametric studies are extended further to examine the effects of ground plane length and the custom-made bioplastic substrate materials on the antenna performance in terms of reflection coefficient. Figure 6 shows the effect of ground plane on the impedance bandwidth and reflection coefficient (S11) of the proposed antenna. Different lengths of the ground plane have been selected and put under investigation to find out the best choice for the proposed antenna. The length of the ground plane has substantial effects on the bandwidth as well as the reflection coefficient. From the basic theory of EM wave propagation of patch antenna, an equal and opposite phase surface current is induced on the ground plane due to the surface currents in the radiating element [17]. Hence, reduced size of ground plane contributes less cross coupling effect and helps to attain considerably larger bandwidth. Through numerical analysis, it has been found that the ground plane length of $L1 = 7.0$ mm which only cover the non-radiating area under the entire length of microstrip line gives widest bandwidth for the proposed design of microstrip antenna.

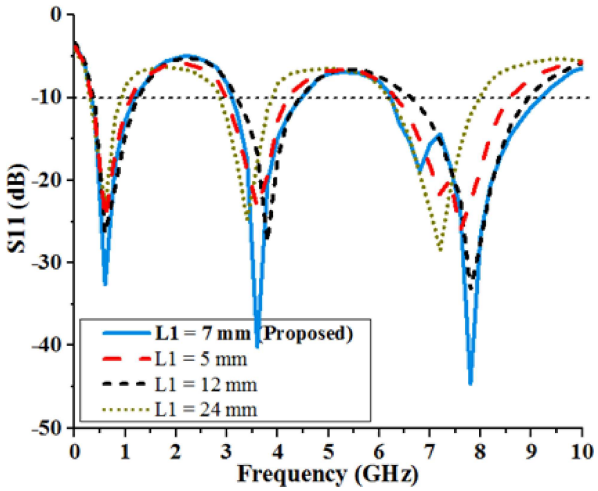

Fig. 6. Effect of ground plane length on the bandwidth and reflection coefficient (S11)

The dielectric properties of the substrate materials greatly affect the antenna size and corresponding operating bandwidth. Substrate material of low dielectric constant value contributes wider bandwidth at the cost of increased overall antenna size and vice versa [1, 18]. Figure 7 exhibits the reflection coefficients of the proposed antenna against the frequency with different types of bioplastic substrate materials. It can be seen from the figure that the bio-10 ($\varepsilon r = 10.0$, $\tan(\delta) = 0.002$) composite material substrate gives better resolution for operating bandwidth and the lowest reflection coefficient value for the proposed antenna structure.

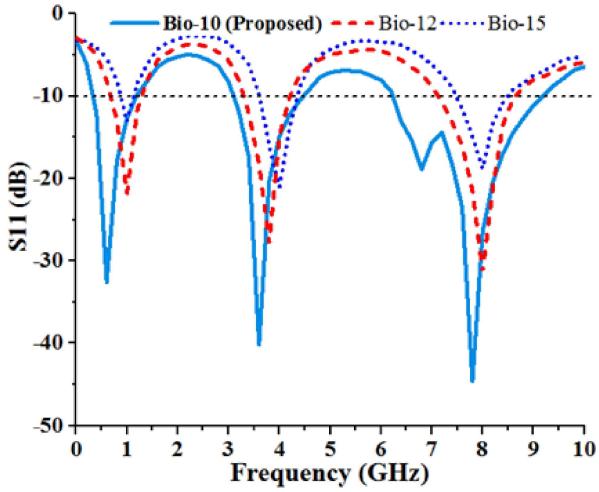

Fig. 7. Effect of substrate materials on the bandwidth and reflection coefficient (S11)

4. Numerical results and discussions

The performance of the multi-band planar antenna has been examined during detail parametric studies by employing HFSS EM simulator. After successful completion of simulation processes, the physical test model of the proposed antenna with optimized parametric dimensions has been fabricated using in-lab LPKF prototyping machine as shown in Fig. 8. The performance of the antenna prototype has been measured in a standard anechoic chamber located at the Faculty of Engineering and Built Environment, Universiti Kebangsaan Malaysia. An Agilent's Precision Vector Network Analyzer E8362C, range up to 20.0 GHz has been used during the entire measurement process. With the aim of providing some testimonies of the consistency and effectiveness of the synthesized multi-band planar antenna, results from the experimental tests and numerical analysis have been compared and discussed in the following.

The measured and simulated values of reflection coefficients (S11) versus frequency of the proposed antenna are given in Fig. 9. The figure clearly shows that the result from the antenna prototype is almost fully compliant with the simulated one and slight variation may arise from some of the factors like SMA soldering, spurious radiation from coaxial cable, fabrication imperfection etc. The Fig. 9 also indicates that the measured -10 dB impedance bandwidths of the proposed antenna are 712 MHz (0.355 to 1.067 GHz), 1.38 GHz (2.92 to 4. GHz) and 2.46 GHz (6.55 to 9.01 GHz) for lower, center and upper operating bands resonate at 0.788 GHz,

3.34 GHz and 8.01 GHz respectively. Considering the impedance bandwidth and the resonance frequency it can be concluded that the proposed antenna is suitable to cover the typical bandwidth requirement for RFID, 3.5 GHz WiMAX band and C/X-band frequencies.

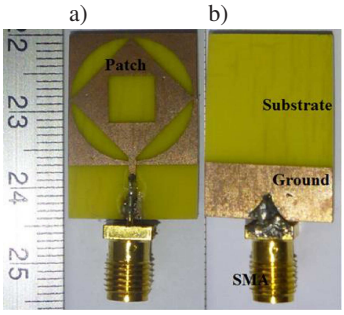

Fig. 8. Photograph of the antenna prototype (a) top view and (b) bottom view

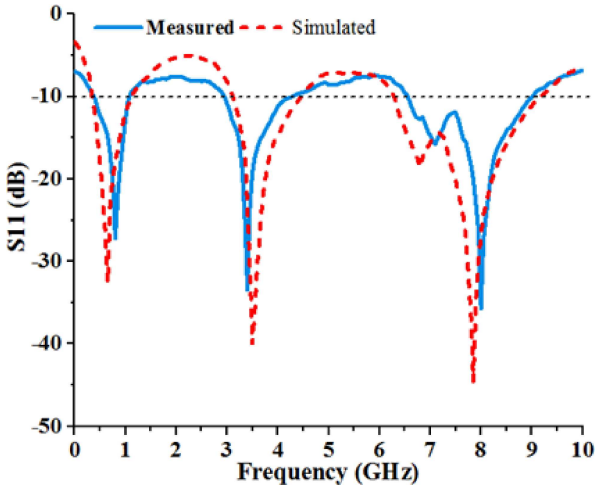

Fig. 9. Simulated and measured amplitude of reflection coefficient (S11) vs frequency of the proposed antenna

To explore the multi-band maneuver mechanism, the simulated surface current distributions of the proposed antenna at resonant modes are shown in Fig. 10. The figure illustrates the surface current distribution excitations at three resonant frequencies of 0.8 GHz, 3.35 GHz and 8.0 GHz are different from each other. At the frequency of 0.8 GHz, the surface current intensity much lower than other two frequencies and mainly concentrated along the outer edge of circle/arc slots and microstrip feed. This clearly establishes that the circular slot dominates the lower resonant frequency. On the other hand, at 3.35 GHz the densities of surface current distribution reaches to higher value and seem to be intensified largely on the surface of inductive loaded rhombus. Hence, we conclude that the inclusion of rhombus as an inductive element for the radiating patch is responsible for creating the middle resonant frequency at around 3.35 GHz. Finally, at 8.0 GHz the current distributions are further amplified than previous frequency which covers significant area of rhombus surface, feed line and top of the patch. This phenomenon certainly justify the wide square slot loading at the center of the patch which perturbed the surface current distribution and accountable for the upper resonant frequency at 8.0 GHz.

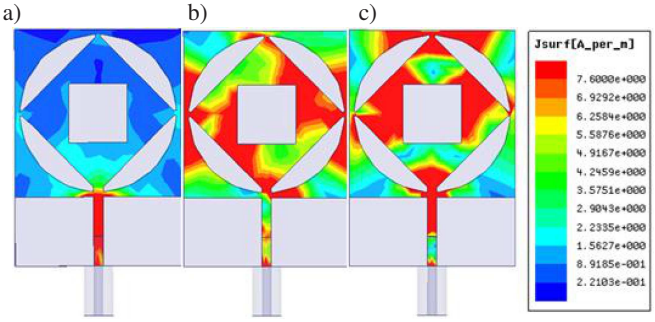

Fig. 10. Distribution of surface currents, simulated at a) 0.8 GHz, b) 3.35 GHz and c) 8.0 GHz

The measured far-field radiation patterns of the proposed antenna in normalized form are presented in Fig. 11 in accordance with two principle planes: E- and H-plane. Here both the co- and cross-polarization patterns are measured at 0.8 GHz, 3.35 GHz and 8.0 GHz, and depicted in the figure. The radiation patterns for both of the planes as seen in the Fig. 10 have almost stable response throughout different operating frequencies and the maximum radiations are seemed to be concentrated along 0 degree. For the operating frequency bands, the E- and H-plane radiation patterns are almost symmetrical and omnidirectional. This may be due to the less cross-polarization effect for both E- and H-plane near the operating frequency bands, the value of which are almost less than -30 dB.

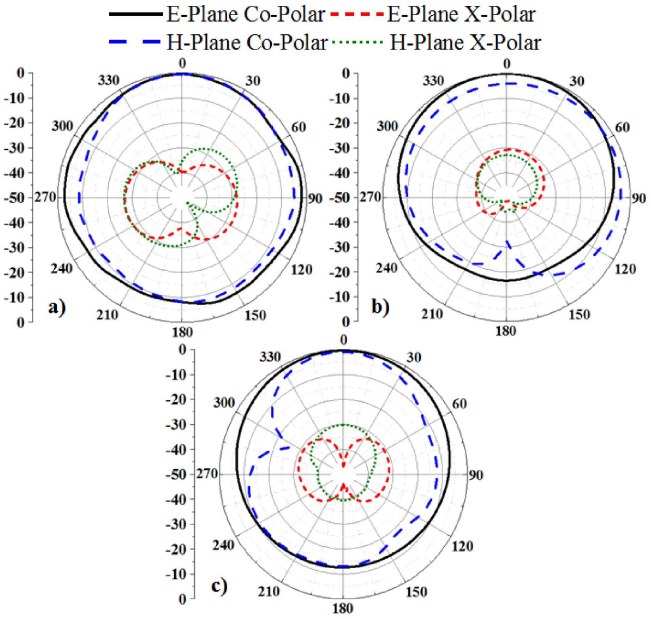

Fig. 11. Measured normalized radiation patterns at a) 0.8 GHz, b) 3.35 GHz and c) 8.0 GHz

The radiation performance of the patch antenna is further numerically verified by measuring the gain where two identical antennas have been used along with the test antenna [19]. The measured gain and corresponding radiating efficiencies of the antenna prototype are depicted in Fig. 12. The

realized gain of the proposed antenna reaches to values of 0.8 dBi at near 0.8 GHz, 2.21 dBi at around 3.35 GHz, and 3.5 dBi at nearby 8.0 GHz. The maximum gains over the three operating bands are observed as 1.37, 2.8 and 3.56 dBi respectively. Meanwhile, it can be noticed that the gain significantly reduces when there is impedance mismatch since most of the EM energy couldn't radiated to the free space. The average radiation efficiencies of the proposed multi-band antenna achieved 76.2%, 78.4% and 81.5% for RFID, 3.5 GHz WiMAX and C/X-band frequency respectively.

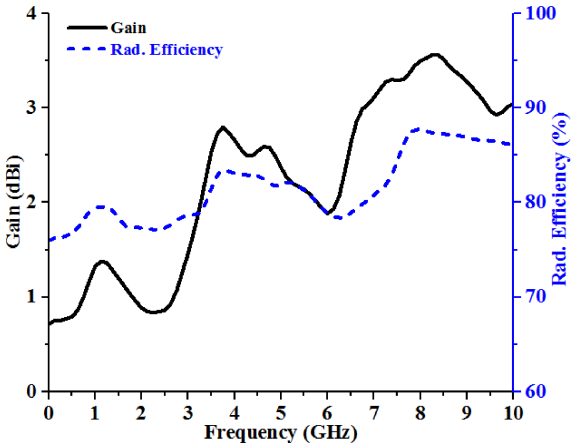

Fig. 12. Measured antenna gain and radiation efficiency of the proposed antenna

5. Conclusions

A simple geometric design of single microstrip line fed rectangular slotted patch antenna has been proposed and the physical module with optimized parameters has been successfully implemented. The design criteria and performance characteristics of the proposed antenna have been investigated through numerical simulations and verified by using experimental data. The results from the parametric analysis and the results of the surface current distribution of the working frequency bands are discussed. The measurement results show that the proposed multi-band antenna has achieved impedance bandwidths of 712 MHz resonates at 0.788 GHz, 1.38 GHz resonates at 3.35 GHz and 2.46 GHz resonates at 8.0 GHz. The proposed multi-band antenna offers considerably symmetrical radiation patterns, almost consistent gain patterns and reasonable radiation efficiencies over the operating frequency bands. The results from antenna prototype affirms that the proposed multi-band planar antenna can be a favorable candidate for providing the wireless communication services for RFID, 3.5 GHz WiMAX and C/X-band applications.

Acknowledgements. The authors would like to acknowledge the support from the University collaboration research grant no: ICONIC-2013-008.

REFERENCES

[1] C.A. Balanis, *Antenna Theory: Analysis and Design*, John Wiley & Sons, Inc., Hoboken, 2005.

[2] M.T. Islam, A.T. Mobashsher, and N. Misran, "Design of microstrip patch antenna using novel U-shaped feeding strip with unequal arm", *Electron. Lett.* 46 (14), 968-970 (2010).

[3] A. Agrawal, P.K. Singhal, and A. Jain, "Design and optimization of a microstrip patch antenna for increased bandwidth", *Int. J. Microw. Wirel. Technol.* 5 (4), 529–535 (2013).

[4] M.R. Ahsan, M.T. Islam, M.H. Ullah, and N. Misran, "Bandwidth enhancement of a dual band planar monopole antenna using meandered microstrip feeding", *Sci. World J.* 2014, 1–8 (2014).

[5] A. Pirhadi, H. Bahrami, and J. Nasri, "Wideband high directive aperture coupled microstrip antenna design by using a FSS superstrate layer", *IEEE Trans. Antennas Propag.* 60 (4), 2101–2106 (2012).

[6] B. Honarbakhsh and A. Tavakoli, "A closed-form spatial green's function for the thick microstrip substrate: The meshless interpolation approach", *Appl. Comput. Electromagn. Soc. J.* 28 (2), 91–98 (2013).

[7] J. Pei, A.-G. Wang, S. Gao, and W. Leng, "Miniaturized triple-band antenna with a defected ground plane for WLAN/WiMAX applications", *IEEE Antennas Wirel. Propag. Lett.* 10, 298–301 (2011).

[8] N.A. Abbasi and R.J. Langley, "Multiband-integrated antenna/artificial magnetic conductor", *IET Microw. Antennas Propag.* 5 (6), 711–717 (2011).

[9] R.S. Aziz, M.A.S. Alkanhal, and A.-F. Sheta, "Multiband fractal-like antennas", *Prog. Electromagn. Res.* B 29, 339–354 (2011).

[10] M.R. Ahsan, M.T. Islam, and M.H. Ullah, "A compact multiband inverted a-shaped patch antenna for WiMAX and C-band", *Microw. Opt. Technol. Lett.* 56 (7), 1540–1543 (2014).

[11] M.H. Ullah, M.T. Islam, J.S. Mandeep, and N. Misran, "A new double L-shaped multiband patch antenna on a polymer resin material substrate", *Appl. Phys. Mater. Sci. Process.* 110 (1), 199–205 (2013).

[12] W. Cao, B. Zhang, A. Liu, T. Yu, D. Guo, and X. Pan, "Multifrequency and dual-mode patch antenna based on Electromagnetic Band-gap (EBG) Structure", *IEEE Trans. Antennas Propag.* 60 (12), 6007–6012 (2012).

[13] B. Li, Z.-H. Yan, T.-L. Zhang, and C. Wang, "Dual-band antenna with U-shaped open stub for WLAN/WiMAX applications", *J. Electromagn. Waves Appl.* 25 (17–18), 2505–2512 (2011).

[14] M.J. Hua, P. Wang, Y. Zheng, and S.L. Yuan, "Compact tri-band CPW-fed antenna for WLAN/WiMAX applications", *Electron. Lett.* 49 (18), 1118–1119 (2013).

[15] W.-C. Liu, C.-M. Wu, and Y. Dai, "Design of triple-frequency microstrip-fed monopole antenna using defected ground structure", *IEEE Trans. Antennas Propag.* 59 (7), 2457–2463 (2011).

[16] *High Frequency Structural Simulator (HFSS)*, ANSYS, Inc., New York, 2015.

[17] M.R. Ahsan, M.H. Ullah, and M.T. Islam, "Slot loaded rectangular patch antenna for dual-band operations on glass-reinforced epoxy laminated inexpensive substrate", *J. Comput. Electron.* 13 (4), 989–995 (2014).

[18] K.R. Carver and J. Mink, "Microstrip antenna technology", *IEEE Trans. Antennas Propag.* 29 (1), 2–24 (1981).

[19] L.V. Blake and M.W. Long, *Antennas: Fundamentals, Design, Measurement*, SciTech Publishing Inc., Raleigh, 2009.